Research Article

Prediction of Metro Train-Induced Tunnel Vibrations Using Machine Learning Method

Zhuosheng Xu,[1,2] Meng Ma [ID],[1,2] Zikai Zhou,[2] Xintong Xie,[2] Haoxiang Xie,[2] Bolong Jiang,[3] and Zhongshuai Zhang[2]

[1]*Key Laboratory of Urban Underground Engineering of Ministry of Education, Beijing Jiaotong University, Beijing 100044, China*
[2]*School of Civil Engineering, Beijing Jiaotong University, Beijing 100044, China*
[3]*National Engineering Research Center of Rail Transit Digital Construction and Measurement Technology,*
 China Railway Design Corporation, Tianjin 300142, China

Correspondence should be addressed to Meng Ma; mameng@bjtu.edu.cn

The tunnel vibration level is usually employed as a vibration source intensity of the empirical prediction method. Currently, the analogy test and data base are two main means to determine the vibration source intensity. To improve the accuracy efficiency, the machine learning (ML) method was introduced to predict the tunnel vibration responses. To acquire model training samples, the measurements were performed in 80 different running tunnel sections of Beijing metro lines. Two types of method, back propagation neural network (BPNN) and generalised regression neural network (GRNN) were employed, which can make full use of characteristics of measured samples and reduce the data noise. The results indicate that the prediction efficiency is high and the mean square errors of the two ML methods are acceptable. Accordingly, both of the ML methods can be used as the reference of vibration source intensity in metro train-induced environmental impact evaluation. GRNN has relatively better predicting ability than BPNN.

1. Introduction

With the development of urban rail transit construction, the environmental vibration problem arising from metro operation is becoming more and more prominent [1–4]. A reasonable vibration mitigation design has put forward higher requirements to the environmental vibration prediction. Various types of prediction model can be employed in different construction stages of a metro project [5, 6]. In the feasibility study stage of developing a rail system, the scoping or preliminary prediction can be used to identify whether the environmental vibration is an issue for potential sensitive buildings along the rail transportation alignment. Empirical and semi-empirical models are widely used in this stage [7–9]. Recently, the machine learning (ML) method has been introduced in the scoping prediction, such as the researches by Paneiro et al. [10], Connolly et al. [11, 12], Chen et al. [13], Yao et al. [14], Paneiro et al. [15], Fang et al.

[16] and Liang et al. [17]. In the scheme design stage, the determined prediction can be used, including various types of numerical [18–22], analytical/semi-analytical methods [23–26]. In the construction design stage, the detail prediction methods were developed, such as measurement-based transfer function method [27–29] and hybrid methods [30–34].

A chain-type formula based on the assumption of uncoupled sub-systems is a classical empirical prediction method. Its idea was originally proposed by Kurzweil [35] and Melke [36], and developed in different standards and guidelines [9, 37–39]. In Chinese code HJ 453-2018 [38], the predicted environmental vibration level VL_z can be calculated by the superposition of the vibration source level $VL_{Z,0}$ and a series of vibration level correction terms, details can be found in reference [40]. The value of $VL_{Z,0}$ is defined as the vertical weighted vibration acceleration level on the tunnel wall. Two main approaches can be used to determine $VL_{Z,0}$.

One is analogy test in a similar running tunnel section, which is regarded as the most accuracy method. Another is searching the database, in which the test has been performed in a similar tunnel section. However, there are disadvantages on both of the methods. The analogy test is time consuming, especially when the workload is heavy. Furthermore, the parameters of the test section should be consistent with the predicted section as far as possible. These parameters include train speed, route radius, tunnel shape and size, track type, soil parameters, etc. It is almost impossible to ensure that all parameters of the two sections are consistent, which introduces errors of the source intensity values. Owing to the large time and labor cost of the analogy test method, the database method is also recommended by standards. However, the database method has the same problem as the analogy test method, and the error is greater because the amount of data available for reference is not large enough.

To solve the problem and improve the prediction efficiency of $VL_{Z,0}$, ML method was introduced in the present study. The in-situ measurements were performed in 80 different tunnel sections of Beijing metro lines and the model training samples of $VL_{Z,0}$ were obtained. Finally, two types of ML method were analysed and the prediction results were validated.

2. Measurement in Metro Tunnel

2.1. Measurement Outline. To obtain the data of $VL_{Z,0}$ for training model, in-situ measurements were performed in 80 different running tunnel sections in Beijing metro. Various types of parameters were obtained and considered for each section, including track type, radius, tunnel shape, train speed and vehicle type, details as:

  (i) Track type: regular slab track, steel spring floating slab track (FST), rubber isolator FST; ladder sleeper track, slab track with short sleeper, and slab track with elastic sleeper;

  (ii) Radius: from 350 m to infinite (straight line);

  (iii) Tunnel shape: horse-shoe tunnel and shield tunnel;

  (iv) Train speed: between 15 and 92 km/h;

  (v) Vehicle type: types A and B.

Figure 1 illustrates the measuring point location in a tunnel with FST. According to the specification HJ 453-2018 [38], the location of the vibration source intensity is defined at the tunnel wall, with 1.25 m height from the rail top. For the curved tunnel, the sensors were installed on the side of inner rails.

In these tests, the date acquisition equipment INV 3060S was employed with a maximum sampling frequency of 51.2 kHz. The accelerometer is Lance 0105T with a measurement range of 20 g and working frequency between 0.35 and 6000 Hz.

2.2. Measurement Result. The vibration source intensity $VL_{Z,0}$ is expressed as the maximum Z-vibration level, defined as:
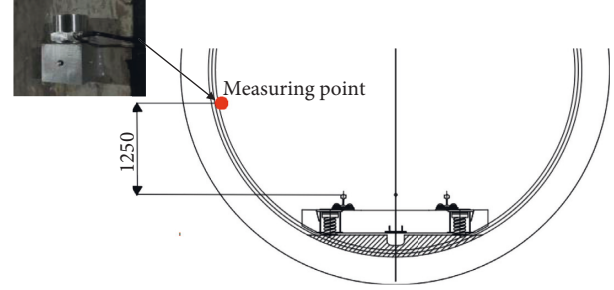

Figure 1: Measuring point location on the tunnel wall (unit: mm).

$$VL_{z,0} = \max_t \left[VL_Z(t) \right] = \max_t \left[20 \lg \frac{a_{w,\tau}(t)}{a_0} \right],$$

$$a_{w,\tau}(t) = \sqrt{\frac{1}{\tau} \int_0^t a_w^2(\xi) \mathrm{d}\xi}, \tag{1}$$

where $VL_z(t)$ is the frequency-weighed vertical vibration acceleration level as a function of time t, $a_{w,\tau}(t)$ is the running root-mean-square weighted acceleration, $a_w(\xi)$ is the frequency-weighed instantaneous vibration acceleration at time ξ, τ is the integration time of the measurement, and t is the instantaneous time. The weighting factor suggested by ISO 2631/1 was employed in this study.

An illustration of the calculation method for maximum Z-vibration level was shown in Figure 2.

All the values of $VL_{Z,0}$ were averaged by five recording pass-by trains. Finally the averaged $VL_{Z,0}$ of the 80 test sections were listed in Table 1. Figure 3 illustrates the $VL_{Z,0}$ of different track type varies with train speeds. Generally, $VL_{Z,0}$ increases with train speed, especially below 40 km/h. Generally speaking, the vibration reduction effect of steel spring FST is better than that of rubber isolator FST. However, sections 10 and 12 were measured in a deep buried horse-shoe tunnel, where the surrounding rock condition and tunnel shape affect the test results of the tunnel responses.

3. Predicting $VL_{z,0}$ Using ML Method

To provide a fast and accuracy prediction of $VL_{z,0}$ based on the measured samples, two types of ML methods were used: back propagation neural network (BPNN) and generalised regression neural network (GRNN).

3.1. BPNN Based Prediction

3.1.1. Method Introduction. BPNN is a type of multilayer feedforward neural network which can acquire output vectors by processing input vectors through hidden layers (Figure 4). The output error can be evaluated by the error function. The error back propagation can be carried out by the gradient descent method based on the output error. Then, the connection weight w_i and threshold b_i between neurons can be modified. Finally, the error of the neural network can be decreased to the minimum. The weight
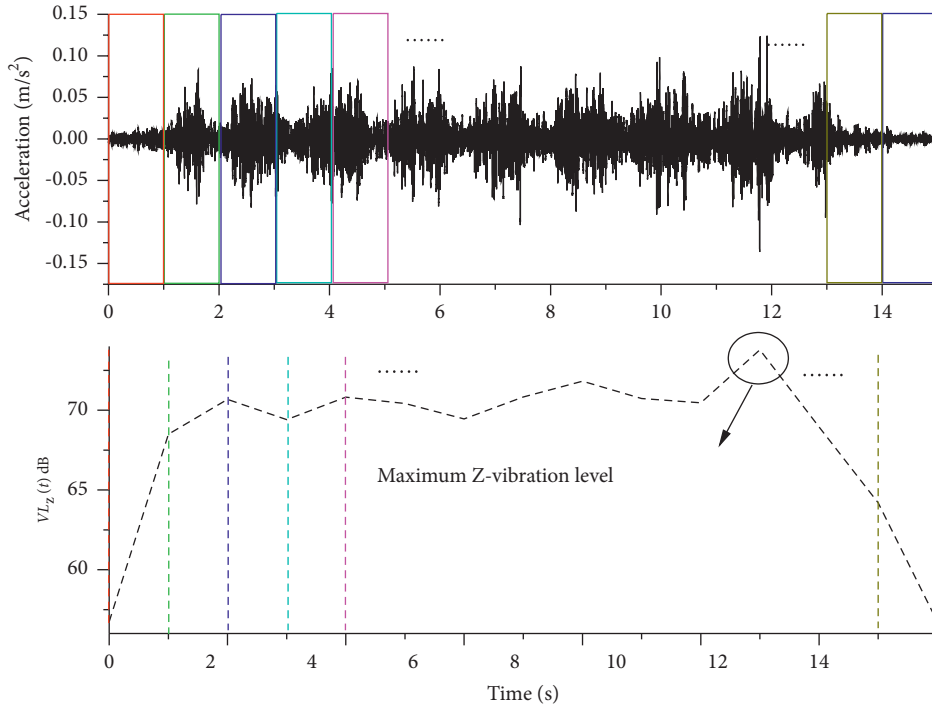
FIGURE 2: Illustration of calculation method for maximum Z-vibration level.

adjustment can be regarded as a prior probability distribution of the weight and threshold. Then, the posterior probability distribution of the weight and threshold are adjusted based on different input data. Finally, the network parameters can be modified and the generalisation ability of network is improved.

The BPNN can be optimised by introducing the Bayes' principle, by which a modification function for the performance function is introduced:

$$F(w) = \alpha E_w + E_d \beta, \tag{2}$$

where, α and β are hyper-parameters; E_w is the network coefficient related to the weight; E_d is the conventional error term. E_w and E_d can be expressed as:

$$E_w = \frac{1}{m} \sum_{i=1}^{m} w_i^2,$$

$$E_D = \frac{1}{N} \sum_{i=1}^{N} [y_i - t_i]^2, \tag{3}$$

where m and N are the neurons number of output and hidden layers, w_i is the initial weight, and y_i is the output vector.

When predicting with BPNN, the initialised weight w_i and hyper-parameters α and β need to be randomised firstly. Subsequently, the training set **P** is input as training samples. After training, the weight w_{MP} is calculated at which the grad of equation (2) is the minimum. Finally, the hyper-parameters can be calculated:

$$a_{MP} = \frac{\gamma}{2E_w(w_{MP})},$$

$$\beta_{MP} = \frac{(N - \gamma)}{2E_D(w_{MP})}, \tag{4}$$

where, γ can be calculated based on w_{MP} and the renewed values of α and β can be re-determined. In equation (5), α_{MP} and β_{MP} are the α and β when w values w_{MP}. The steps above are repeated until the network converge [41].

According to the number of data eigenvalues, six nodes were set in the input layer, and the network layer number was set as 3 to lower the complexity of network and pretend over-fitting. One node was set in the output layer, and output value was the predicted vibration source intensity, e.g. maximum Z-vibration level.

The mean squared error (MSE) was used to analyse the prediction performance of the network. MSE is defined as:

$$MSE = \frac{1}{n} \sum_{i=1}^{N} (\hat{y}_i - y_i)^2, \tag{5}$$

where y_i and $\hat{y}_i$ are the true and predicted values of the test set, respectively; N is the number of output layer.

In this study, the value of $VL_{Z,0}$ is expressed in dB, so MSE is measured in dB^2. Generally, the $VL_{Z,0}$ is between 60 and 80 dB. If the predicted average percentage error is 10%, the absolute error is approximately between 6 and 8 dB. That is, if MSE is below 36 dB^2, it can be regarded as an acceptable result.

TABLE 1: Average source intensity and parameter of 80 sections.

Test section nr.	Track type	Radius (m)	Tunnel type	Speed (km/h)	Vehicle type	Average $VL_{z,0}$ (dB)
1	Regular slab track	650	Shield tunnel	70	B	77.8
2	Steel spring FST	650	Shield tunnel	70	B	60.53
3	Steel spring FST	Straight line	Shield tunnel	70	B	59.5
4	Regular slab track	Straight line	Shield tunnel	70	B	80
5	Steel spring FST	Straight line	Shield tunnel	70	B	64.5
6	Steel spring FST	Straight line	Shield tunnel	70	B	66
7	Regular slab track	Straight line	Shield tunnel	75	B	64.7
8	Steel spring FST	450	Horse-shoe tunnel	59.8	B	45.1
9	Regular slab track	450	Horse-shoe tunnel	64.7	B	66.2
10	Rubber isolator FST	490	Horse-shoe tunnel	75.4	B	51.9
11	Regular slab track	505	Horse-shoe tunnel	66.2	B	64.9
12	Rubber isolator FST	505	Horse-shoe tunnel	77.5	B	52.4
13	Regular slab track	505	Horse-shoe tunnel	66.2	B	64.9
14	Ladder sleeper track	Straight line	Shield tunnel	57.8	B	68.9
15	Regular slab track	Straight line	Shield tunnel	60.4	B	82.5
16	Steel spring FST	650	Shield tunnel	88	B	73.63
17	Steel spring FST	650	Shield tunnel	92	B	73.56
18	Ladder sleeper track	650	Shield tunnel	90	B	88.75
19	Ladder sleeper track	Straight line	Shield tunnel	90	B	79.96
20	Ladder sleeper track	650	Shield tunnel	75	B	82.91
21	Ladder sleeper track	1156	Shield tunnel	87	B	75.93
22	Slab track with short sleeper	350	Shield tunnel	15	B	68
23	Slab track with short sleeper	Straight line	Shield tunnel	15	B	65.2
24	Slab track with short sleeper	Straight line	Shield tunnel	15	B	61.2
25	Steel spring FST	Straight line	Shield tunnel	15	B	47
26	Slab track with elastic long sleeper	350	Shield tunnel	15	B	63.2
27	Steel spring FST	Straight line	Shield tunnel	15	B	53.1
28	Slab track with short sleeper	350	Shield tunnel	25	B	74
29	Slab track with short sleeper	Straight line	Shield tunnel	25	B	67.2
30	Slab track with short sleeper	Straight line	Shield tunnel	25	B	59.2
31	Steel spring FST	Straight line	Shield tunnel	25	B	50.5
32	Slab track with elastic long sleeper	350	Shield tunnel	25	B	69.1
33	Slab track with elastic long sleeper	500	Shield tunnel	25	B	68.1
34	Slab track with elastic long sleeper	Straight line	Shield tunnel	25	B	60.9
35	Steel spring FST	Straight line	Shield tunnel	25	B	58.8
36	Slab track with short sleeper	350	Shield tunnel	35	B	76.3
37	Slab track with short sleeper	Straight line	Shield tunnel	35	B	77.6
38	Slab track with short sleeper	Straight line	Shield tunnel	35	B	69.5
39	Steel spring FST	Straight line	Shield tunnel	35	B	54.5
40	Slab track with elastic long sleeper	350	Shield tunnel	35	B	74.7
41	Slab track with elastic long sleeper	500	Shield tunnel	35	B	80.7
42	Slab track with elastic long sleeper	Straight line	Shield tunnel	35	B	70.5
43	Steel spring FST	Straight line	Shield tunnel	35	B	55.6
44	Slab track with short sleeper	350	Shield tunnel	45	B	78.7
45	Slab track with short sleeper	Straight line	Shield tunnel	45	B	81.7
46	Slab track with short sleeper	Straight line	Shield tunnel	45	B	71.8
47	Steel spring FST	Straight line	Shield tunnel	45	B	56.3
48	Slab track with elastic long sleeper	350	Shield tunnel	45	B	74.8
49	Slab track with elastic long sleeper	500	Shield tunnel	45	B	78.2
50	Slab track with elastic long sleeper	Straight line	Shield tunnel	45	B	72.8
51	Steel spring FST	Straight line	Shield tunnel	45	B	57.4
52	Slab track with short sleeper	350	Shield tunnel	57	B	81.4
53	Slab track with short sleeper	Straight line	Shield tunnel	57	B	82.4
54	Slab track with short sleeper	Straight line	Shield tunnel	57	B	72.6
55	Steel spring FST	Straight line	Shield tunnel	57	B	57.2
56	Slab track with elastic long sleeper	350	Shield tunnel	57	B	74.6
57	Slab track with elastic long sleeper	500	Shield tunnel	57	B	77.2
58	Slab track with elastic long sleeper	Straight line	Shield tunnel	57	B	71.3
59	Steel spring FST	Straight line	Shield tunnel	57	B	57.4
60	Ladder sleeper track	Straight line	Horse-shoe tunnel	64	B	68.795

Table 1: Continued.

Test section nr.	Track type	Radius (m)	Tunnel type	Speed (km/h)	Vehicle type	Average $VL_{z,0}$ (dB)
61	Ladder sleeper track	Straight line	Horse-shoe tunnel	64	B	68.63
62	Regular slab track	Straight line	Shield tunnel	67.7	B	83
63	Steel spring FST	350	Shield tunnel	45	B	61.5
64	Ladder sleeper track	Straight line	Shield tunnel	60.6	B	71.5
65	Steel spring FST	Straight line	Shield tunnel	75	B	64.5
66	Steel spring FST	Straight line	Horse-shoe tunnel	68.6	B	61.5
67	Steel spring FST	Straight line	Horse-shoe tunnel	67.6	B	68
68	Regular slab track	Straight line	Horse-shoe tunnel	68.3	B	78
69	Regular slab track	Straight line	Horse-shoe tunnel	69.3	B	68
70	Regular slab track	Straight line	Shield tunnel	69.4	B	78
71	Regular slab track	Straight line	Shield tunnel	36	B	81.2
72	Regular slab track	Straight line	Shield tunnel	40	B	84.9
73	Regular slab track	Straight line	Shield tunnel	69	B	85.9
74	Regular slab track	Straight line	Shield tunnel	76	B	82
75	Regular slab track	Straight line	Shield tunnel	78	B	81.6
76	Regular slab track	Straight line	Shield tunnel	69	B	85.8
77	Regular slab track	Straight line	Shield tunnel	69	B	78.8
78	Regular slab track	Straight line	Shield tunnel	72	B	79.7
79	Regular slab track	Straight line	Shield tunnel	68	A	84.5
80	Regular slab track	Straight line	Shield tunnel	68	A	87.5
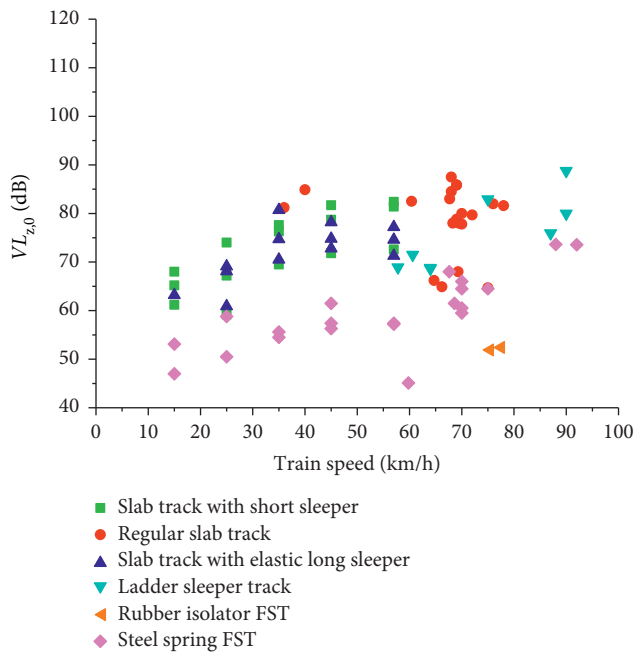
Figure 3: Tunnel vibration responses vary with train speed.

- ■ Slab track with short sleeper
- ● Regular slab track
- ▲ Slab track with elastic long sleeper
- ▼ Ladder sleeper track
- ◀ Rubber isolator FST
- ◆ Steel spring FST

The relationship between node number of hidden layers, eigenvalue number and input/output node number can be expressed as [42].

$$s = \sqrt{m + n} + a, \tag{6}$$

where s and m are node numbers of the hidden layer and input layer.

3.1.2. Sample Training and Results. According to equation (6), the test begins with three nodes of the hidden layers. With the same training set and test set, the node number of the hidden layer can be increased gradually. The training is

repeated three times for each hidden layer, and the averaged value can be obtained. The training results are illustrated in Figure 5 and the final optimised node number was six.

The model was building using the neural network toolbox in MATLAB. The activation function for the hidden layer was Sigmod function and for the output layer was purelin function. The maximum convergence times was set as 1000, and the maximum training accuracy was 0. The Bayesian regularisation method (trainbr) was selected as the training method. A total of eight groups of data were randomly selected for test and the rest 72 groups of data were used as the train set. After training the neural network with the train set, the test set was predicted.

When training, a weight matrix was randomly generated and then weight was modified with the transmission error.

Figure 6 illustrates the training results by comparing measured and predicted values. Based on equation (5), MSE of this test set can be calculated as 29.98, which proves the accuracy of training model is good enough to perform the prediction. According to detailed information in Figure 6, the absolute error of MSE is controlled within 10%, ranging from −7.57% to 9.86%, which demonstrates an acceptable prediction ability of this model.

3.1.3. Test and Verification. To ensure the generalisation ability of the network, a cross validation was performed. After arranging data randomly, the data were divided into ten subsets. Every subset was selected as a test set, and the remaining were training sets. The cross validation were repeated ten times following the above steps. Figure 7 demonstrates MSE of ten cross validation results and the averaged MSE is 32.28, which demonstrates a good generalisation ability of this method.

Furthermore, the method of leave-one-out-cross-validation (LOOCV) was used to calculate and analyse the errors between measured and predicted values. Figure 8
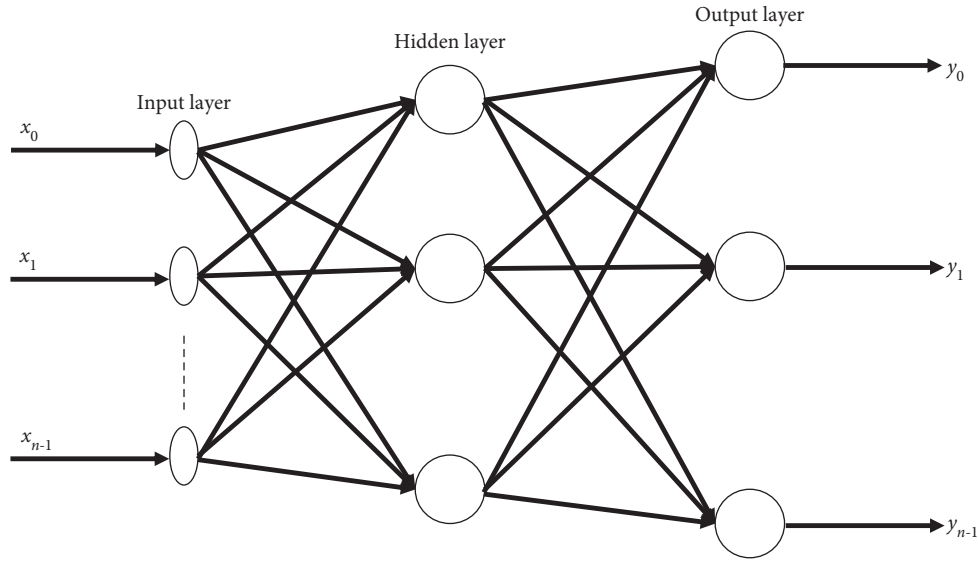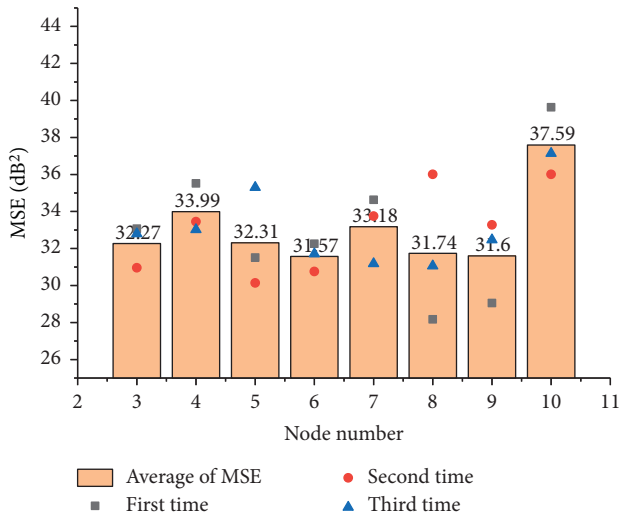
FIGURE 4: Topology of BPNN.

FIGURE 5: MSE of different node number of hidden layer.

FIGURE 6: Predicted result of back propagation neural network.

illustrates the error normal distribution of BPNN using LOOCV.

Based on the verification of LOOCV and cross validation, the prediction error is generally below 10% and the average MSE is less than 35. Accordingly, BPNN can be used to undertake a preliminary prediction of the source intensity vibration of a running metro train.

Moreover, coefficient of determination R^2 can be used to evaluate linear correlation degree of network fitting result. The coefficient of determination is defined as

$$R^2 = \frac{\text{SSR}}{\text{SST}},$$
$$\text{SSR} = \sum_i (\hat{y}_i - \overline{y}_i)^2, \quad (7)$$
$$\text{SST} = \sum_i (y_i - \overline{y}_i)^2,$$

where, y_i is the true value, $\hat{y}_i$ is the predicted value, and $\overline{y}_i$ is the average of true value.

Coefficient of determination R^2 ranges from 0 to 1. The closer R^2 approaches to 1, the better the linear correlation degree of network fitting result is. After calculation, R^2 of BPNN is 0.9464, which reflects the BPNN model can also be used to predict the vibration source intensity.

3.2. GRNN Based Prediction

3.2.1. Method Introduction. GRNN is a type of radial basis function (RBF) neural network, which has strong non-linear mapping capability, fault tolerance and robustness. Besides, it has the advantage in the approaching ability and learning speed. The model of radial basis neural network includes two main independent variable and basis function. The
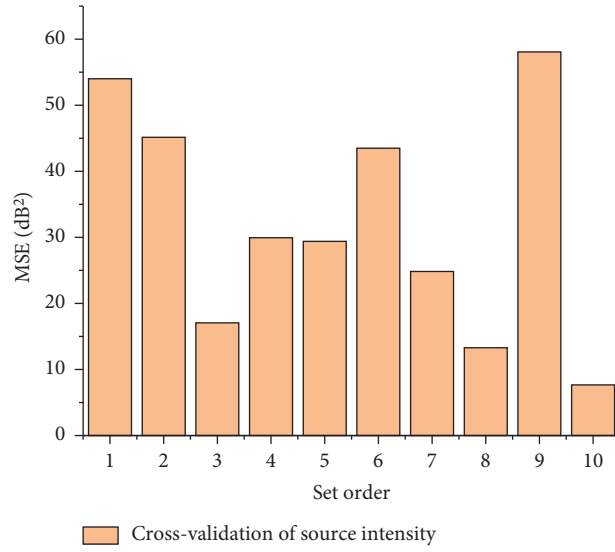
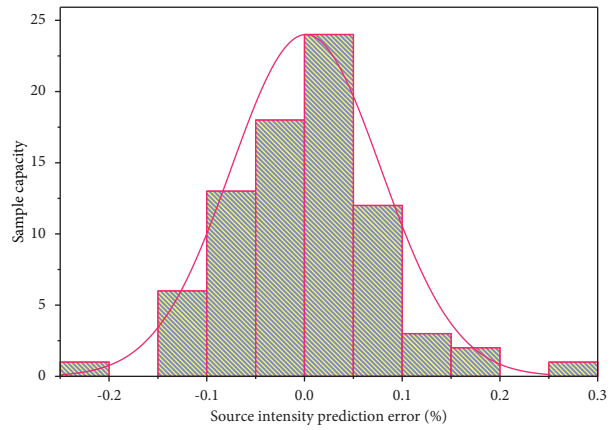FIGURE 7: Cross validation of source intensity prediction.

FIGURE 8: Error distribution of vibration source intensity predicted using BPNN.
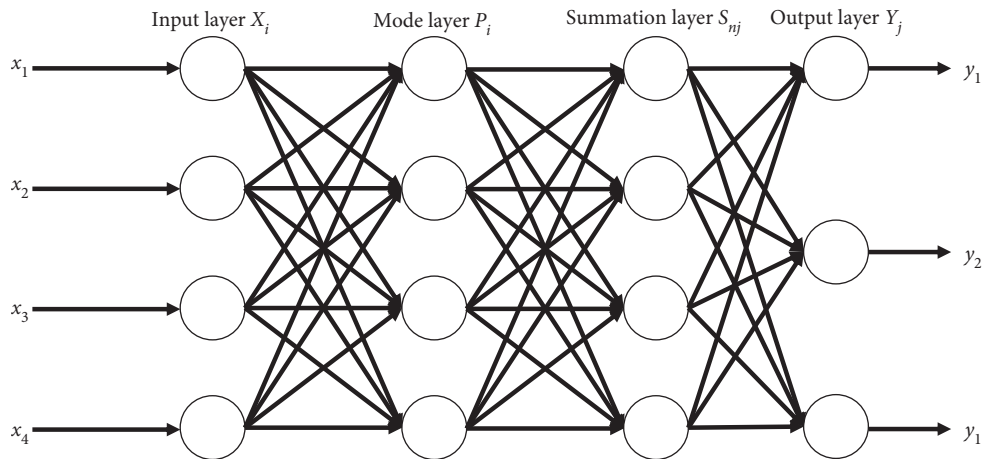

FIGURE 9: Topology of GRNN.

independent variable is the Euclidean distance between the points to be measured and sampling. The basis function is a radial function. GRNN can transform a multi-dimensional problem into a one-dimensional problem. After transformation, the independent variable of one-dimensional issue turns into the Euclidean distance mentioned above. Any function can be obtained by making weighted combination of basis functions. Figure 9 demonstrates the topology of GRNN.

In the calculation and analyse by GRNN, the training set **P** is firstly input as a learning sample, and then S_D and S_{Ni} are calculated and output to the summation layer. S_D and S_{Ni} are neurons in the hidden layer, calculated by two different methods. One is the summation of denominator neurons, i.e. straightly summing up all the neurons in hidden layers. The other is the summation of molecular neurons, i.e. making a weighted summation of neurons in mode layers. S_D and S_{Ni} can be calculated by

$$S_D = \sum_{i=1}^{n} P_i = \sum_{i=1}^{n} \exp\left[\frac{(x-x_i)^T(x-x_i)}{2\sigma_i^2}\right], i = 1, 2, 3 \ldots n,$$

$$S_{N_i} = \sum_{i=1}^{n} Y_i P_i = \sum_{i=1}^{n} y_{ij} \exp\left[\frac{(X-X_i)^T(X-X_i)}{2\sigma_i^2}\right], j = 1, 2, 3 \ldots n, \tag{8}$$

where σ_i is a network expansion constant, y_{ij} is the connecting weight of the i-th neuron in the summation layer and the j-th neuron in the mode layer. Finally, the output network predicted value can be obtained: $y_j = S_D/S_{Ni}$ [43].

According to the characteristic of RBF neural network, the data should be expressed in the form of scientific counting before normalisation. Then, the route radius was multiplied by 0.01 and the train speed was multiplied by 0.1. Based on the fast learning speed of GRNN, building a large network and performing mutual authentications are possible. Then, the network was built for all 80 groups of data one by one. The i-th group of data was selected as the test set and the remaining were the train sets. Thus, a total of 80 networks can be established and the data can be made full used.

3.2.2. Results, Test and Verification. After training, 80 groups of predicted results can be obtained using LOOCV. Figure 10 demonstrates the comparison between predicted and measured values.

Figure 11 demonstrates MSE values under different values of σ. According to Figure 11, the value of σ have little influence on the result of this experiment. When $\sigma = 1$ the MSE value is the minimum. Accordingly, this value was determined in this experiment.

Both of the MSE and coefficient of determination R^2 were used to evaluate linear correlation degree of network fitting result. After calculation, MSE is 17.9205, and R^2 is 0.8153. Figure 12 demonstrates the error distribution. For its normal fitting curve, average value is 0.004664 and standard deviation is 0.07571.

The above results and verification proves that GRNN can be used to predict the vibration source intensity with considering different parameters. Compared with BPNN,
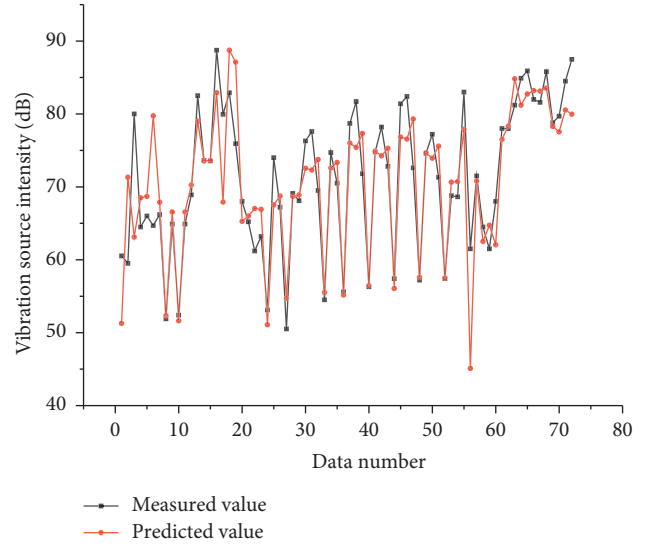

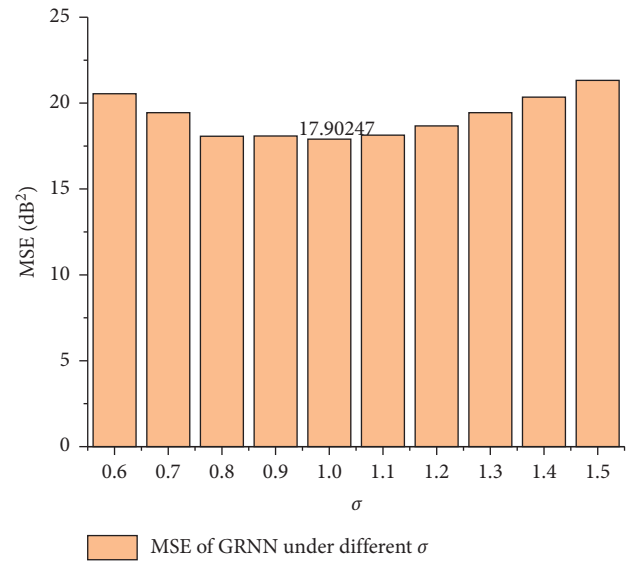FIGURE 10: GRNN based predicted result.

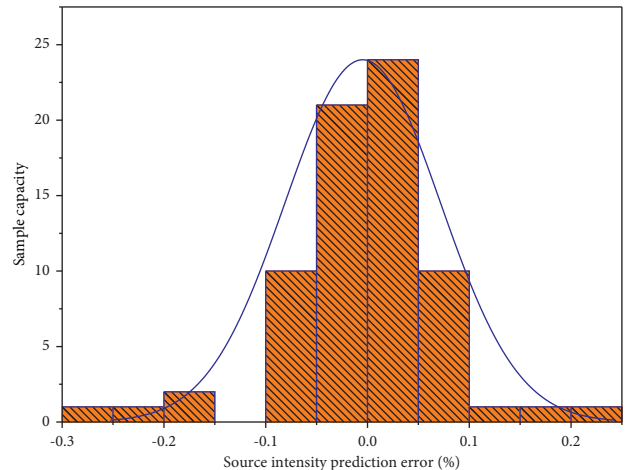FIGURE 11: MSE of GRNN under different values of σ.

FIGURE 12: Source intensity prediction error distribution predicted by GRNN.

both of the calculation efficiency and the accuracy of GRNN are higher. Accordingly, GRNN is more recommended to predict the vibration source intensity.

4. Conclusion

To improve the prediction efficiency of $VL_{Z,0}$ in the empirical prediction formula, ML method was introduced in the present study. In-situ measurements were performed in 80 different running tunnel sections of Beijing metro and the model training samples of $VL_{Z,0}$ were obtained. Two types of ML method were employed and compared for the prediction results. The results indicate that:

(1) Both of BPNN and GRNN can be used to predict the tunnel vibration responses $VL_{Z,0}$. Proved by LOOCV, predicting by neural network has good extensionality. In the preliminary prediction phase, the neural network based prediction results can be used as reference values in the preliminary prediction.

(2) GRNN has relatively better predicting ability than BPNN.

This study only explores the application of ML for predicting $VL_{Z,0}$. As the number and quality of test samples used for training determine the accuracy of prediction results, more test work is suggested to be carried out in future to enrich training samples.

Data Availability

The data used to support the findings of this study are available from the corresponding author upon request.

Conflicts of Interest

The authors declare that they have no conflicts of interest.

Acknowledgments

References

[1] J. J. Yang, S. Y. Zhu, W. M. Zhai et al., "Prediction and mitigation of train-induced vibrations of large-scale building constructed on subway tunnel," *Science of the Total Environment*, vol. 668, pp. 485–499, 2019.

[2] T. Xin, S. Wang, L. Gao et al., "Field measurement of rail corrugation influence on environmental noise and vibration: a case study in China," *Measurement*, vol. 164, Article ID 108084, 2020.

[3] C. He, S. Zhou, and P. Guo, "An efficient three-dimensional method for the prediction of building vibrations from underground railway networks," *Soil Dynamics and Earthquake Engineering*, vol. 139, Article ID 106269, 2020.

[4] L. H. Xu, M. Ma, R. N. Cao, X. Y. Tan, and R. H. Liang, "Effect of longitudinally varying characteristics of soil on metro train-induced ground vibrations based on wave propagation analysis," *Soil Dynamics and Earthquake Engineering*, vol. 152, Article ID 107020, 2022.

[5] ISO Standard, "Mechanical vibration – ground-borne noise and vibration arising from rail system—part 1: general guidance," ISO Standard, Geneva, Switzerland, ISO 14837-1, 2005.

[6] M. Ma, W. N. Liu, and W. F. Liu, "Research progresses of prediction method and uncertainty of train-induced environmental vibration," *Journal of Traffic and Transportation Engineering*, vol. 20, pp. 1–17, 2020.

[7] C. With, M. Bahrekazemi, and A. Bodare, "Validation of an empirical model for prediction of train-induced ground vibrations," *Soil Dynamics and Earthquake Engineering*, vol. 26, no. 11, pp. 983–990, 2006.

[8] C. Madshus, B. Bessason, and L. Hårvik, "Prediction model for low frequency vibration from high speed railways on soft ground," *Journal of Sound and Vibration*, vol. 193, no. 1, pp. 195–203, 1996.

[9] M. Bahrekazemi, *Train-induced Ground Vibration and its Prediction*, Royal institute of technology, Stockholm, Sweden, 2004.

[10] G. Paneiro, F. O. Durão, M. Costa e Silva, P. Falcão Neves, and P. Neves, "Prediction of ground vibration amplitudes due to urban railway traffic using quantitative and qualitative field data," *Transportation Research Part D: Transport and Environment*, vol. 40, pp. 1–13, 2015.

[11] D. P. Connolly, G. Kouroussis, A. Giannopoulos, O. Verlinden, P. K. Woodward, and M. C. Forde, "Assessment of railway vibrations using an efficient scoping model," *Soil Dynamics and Earthquake Engineering*, vol. 58, pp. 37–47, 2014.

[12] D. P. Connolly, G. Kouroussis, O. Verlinden, A. Giannopoulos, P. K. Woodward, and M. C. Forde, "Scoping prediction of re-radiated ground-borne noise and vibration near high speed rail lines with variable soils," *Soil Dynamics and Earthquake Engineering*, vol. 66, pp. 78–88, 2014.

[13] Y. J. Chen, C. J. Chen, and Y. J. Shen, "Development of automatic prediction model for ground vibration using support vector machine," *Journal of Vibroengineering*, vol. 17, no. 5, pp. 2535–2546, 2015.

[14] J. B. Yao, H. Xia, N. Zhang, and B. Yu, "Prediction on building vibration induced by moving train based on support vector machine and wavelet analysis," *Journal of Mechanical Science and Technology*, vol. 28, no. 6, pp. 2065–2074, 2014.

[15] G. Paneiro, F. O. Durão, M. Costa e Silva, and P. Falcão Neves, "Artificial neural network model for ground vibration amplitudes prediction due to light railway traffic in urban areas," *Neural Computing & Applications*, vol. 29, no. 11, pp. 1045–1057, 2018.

[16] L. Fang, J. B. Yao, and H. Xia, "Prediction on soil-ground vibration induced by high-speed moving train based on artificial neural network model," *Advances in Mechanical Engineering*, vol. 11, no. 5, Article ID 168781401984729, 2019.

[17] R. H. Liang, W. F. Liu, M. Ma, and W. N. Liu, "An Efficient model for predicting the train-induced ground-borne vibration and uncertainty quantification based on Bayesian neural network," *Journal of Sound and Vibration*, vol. 495, Article ID 115908, 2021.

[18] P. Amado-Mendes, P. Alves Costa, L. M. C. Godinho, and P. Lopes, "2.5D MFS-FEM model for the prediction of vibrations due to underground railway traffic," *Engineering Structures*, vol. 104, no. 1, pp. 141–154, 2015.

[19] M. Ma, W. N. Liu, C. Y. Qian, G. H. Deng, and Y. Li, "Study of the train-induced vibration impact on a historic Bell Tower above two spatially overlapping metro lines," *Soil Dynamics and Earthquake Engineering*, vol. 81, pp. 58–74, 2016.

[20] Q. Jin, D. J. Thompson, D. E. Lurcock, M. G. R. Toward, and E. Ntotsios, "A 2.5D finite element and boundary element model for the ground vibration from trains in tunnels and validation using measurement data," *Journal of Sound and Vibration*, vol. 422, pp. 373–389, 2018.

[21] C. He, S. H. Zhou, P. J. Guo, H. G. Di, and X. H. Zhang, "Modelling of ground vibration from tunnels in a poroelastic half-space using a 2.5-D FE-BE formulation," *Tunnelling and Underground Space Technology*, vol. 82, pp. 211–221, 2018.

[22] M. Ma, L. H. Xu, L. L. Du, Z. Z. Wu, and X. Y. Tan, "Prediction of building vibration induced by metro trains running in a curved tunnel," *Journal of Vibration and Control*, vol. 27, no. 5-6, pp. 515–528, 2021.

[23] S. H. Zhou, X. H. Zhang, H. G. Di, and C. He, "Metro train-track-tunnel-soil vertical dynamic interactions - semi-analytical approach," *Vehicle System Dynamics*, vol. 56, no. 12, pp. 1945–1968, 2018.

[24] Z. Yuan, Z. Cao, A. Boström, and Y. Q. Cai, "The influence of pore-fluid in the soil on ground vibrations from a tunnel embedded in a layered half-space," *Journal of Sound and Vibration*, vol. 419, pp. 227–248, 2018.

[25] Z. Yuan, A. Boström, Y. Q. Cai, X. D. Pan, Z. G. Cao, and L. Shi, "The wave function method for calculation of vibrations from a twin tunnel in a multi-layered half-space," *Soil Dynamics and Earthquake Engineering*, vol. 125, Article ID 105716, 2019.

[26] L. H. Xu and M. Ma, "Dynamic response of the multilayered half-space medium due to the spatially periodic harmonic moving load," *Soil Dynamics and Earthquake Engineering*, vol. 157, Article ID 107246, 2022.

[27] N. Zhang, H. Xia, W. G. Yang, and S. Y. Zhao, "Prediction and control of building vibration under metro excitations," in *Proceedings of the 8th International Conference on Structural Dynamics*, pp. 705–711, Leuven, Belgium, July 2011.

[28] T. Jaquet and V. Salcedo, "Ensuring acceptable vibration levels in listed buildings by means of precise vibration measurements and highly-efficient floating slab track," in *Proceedings of the AREMA. 2012 Annual Conference and Exposition*, pp. 1–11, Atlanta, GA, USA, June 2012.

[29] W. F. Liu, Z. Z. Wu, C. Y. Li, and L. H. Xu, "Prediction of ground-borne vibration induced by a moving underground train based on excitation experiments," *Journal of Sound and Vibration*, vol. 523, Article ID 116728, 2022.

[30] H. Verbraken, G. Lombaert, and G. Degrande, "Verification of an empirical prediction method for railway induced vibrations by means of numerical simulations," *Journal of Sound and Vibration*, vol. 330, no. 8, pp. 1692–1703, 2011.

[31] H. Verbraken, *Prediction of Railway Induced Vibration by Means of Numerical, Empirical, and Hybrid Methods*, University of Southampton, Southampton, UK, 2013.

[32] K. A. Kuo, H. Verbraken, G. Degrande, and G. Lombaert, "Hybrid predictions of railway induced ground vibration using a combination of experimental measurements and numerical modelling," *Journal of Sound and Vibration*, vol. 373, pp. 263–284, 2016.

[33] K. A. Kuo, G. D. Lombaert, and G. Degrande, "Quantifying dynamic soil-structure interaction for railway induced vibrations," *Procedia Engineering*, vol. 199, pp. 2372–2377, 2017.

[34] G. Kouroussis, K. E. Vogiatzis, and D. P. Connolly, "Assessment of railway ground vibration in urban area using in-situ transfer mobilities and simulated vehicle-track interaction," *International Journal of Reality Therapy*, vol. 6, no. 2, pp. 113–130, 2018.

[35] L. G. Kurzweil, "Ground-borne noise and vibration from underground rail systems," *Journal of Sound and Vibration*, vol. 66, no. 3, pp. 363–370, 1979.

[36] J. Melke, "Noise and vibration from underground railway lines: proposals for a prediction procedure," *Journal of Sound and Vibration*, vol. 120, no. 2, pp. 391–406, 1988.

[37] A. Koopman, S. Lentzen, R. Steenbergen R, A. V. Metrikine, J. S. Hoving, and Srm-T, "The Dutch standardized prediction model for railway vibration and induced noise," in *Proceedings of the 4th International Symposium on Environmental Vibration (ISEV2009)*, vol. 86, Beijing, China, December 2009.

[38] Chinese code of Ecology & Environment, "Technical guidelines for environmental impact assessment – urban rail transit," Chinese code of Ecology & Environment, Beijing, China, Hj 453-2018(in Chinese), 2018.

[39] Chinese Industry Standard, "Code for application technique of metro noise and vibration control," Chinese Industry Standard, Beijing, China, DB11/T 838-2019(in Chinese), 2019.

[40] M. Ma, M. H. Li, X. Y. Qu, and H. G. Zhang, "Effect of passing metro trains on uncertainty of vibration source intensity: monitoring tests," *Measurement*, vol. 193, Article ID 110992, 2022.

[41] D. Wei, M. L. Zhang, Z. J. Jiang, and M. Sun, "Neural network non-linear modelling based on Bayesian methods," *Computer Engineering and Applications*, vol. 11, pp. 5–8, 2005.

[42] D. H. Qi and J. C. Kang, "Design of back propagation neural network," *Computer Engineering and Design*, vol. 2, pp. 47–49, 1998.

[43] J. Yang and Z. G. Yang, "Non-intrusive load monitoring method aircraft electrical equipment based on GRNN algorithm," *Acta Aeronautica et Astronautica Sinica*, vol. 42, no. 3, pp. 403–413, 2020.